View metadata, citation and similar papers at core.ac.uk
brought to you by CORE
provided by Elsevier - Publisher Connector

Chinese Journal of Aeronautics 24 (2011) 90-95

Contents lists available at ScienceDirect

Chinese Journal of Aeronautics

journal homepage: www.elsevier.com/locate/cja

Surface Roughness Effects on Vortex Torque of Air Supported Gyroscope

LIANG Yingchun*, LIU Jingshi, SUN Yazhou, LU Lihua

School of Mechatronics Engineering, Harbin Institute of Technology, Harbin 150001, China

Received 9 March 2010; revised 21 May 2010; accepted 21 June 2010

Abstract

In order to improve the drift precision of air supported gyroscope, effects of surface roughness magnitude and direction on vortex torque of air supported gyroscope are studied. Based on Christensen's rough surface stochastic model and consistency transformation method, Reynolds equation of air supported gyroscope containing surface roughness information is established. Also effects of mathematical models of main machining errors on vortex torque are established. By using finite element method, the Reynolds equation is solved numerically and the vortex torque in the presence of machining errors and surface roughness is calculated. The results show that surface roughness of slit has a significant effect on vortex torque. Transverse surface roughness makes vortex torque greater, while longitudinal surface roughness makes vortex torque smaller. The maximal difference approaches 11.4% during the range analyzed in this article. However surface roughness of journal influences vortex torque insignificantly. The research is of great significance for designing and manufacturing air supported gyroscope and predicting its performance.

Keywords: air supported gyroscope; surface roughness; Christensen's stochastic model; consistency transformation; vortex torque

1. Introduction

The precision of inertial navigation and guidance system is the most important target evaluating the quality of inertial navigation and guidance system, while the precision of gyroscope determines the precision of inertial navigation and guidance system to a great extent[1]. Air supported gyroscope is ultra precision inertial instrument. Since it is influenced by complicated and wicked mechanical environment such as vibration and shock as the work proceeds, how to effectively increase the precision of air supported gyroscope becomes key problem of its development.

Aerostatic bearing is an important part of inertial instrument, and its performance determines the precision of the inertial instrument. Vortex torque is a spin torque caused by tangential distributary on the journal surface, and the tangential distributary is caused by the non-uniform gas flow going through the throttling slit under the circumstances of zero bearing speed[2]. It is an important factor evaluating the hydrostatic bearing performance[3], and it is also the major disturbing torque affecting the drift precision of air supported gyroscope. There are many factors causing vortex torque. Generally speaking, all machining errors and structure factors causing asymmetric tangential flow between the bearing clearance are immediate cause of vortex torques. In practice, the major factors affecting the vortex torque are machining errors such as roundness error of journal surface and tilting error of throttling slit[4]. Du[5-6] and Liu[7-8], et al. studied the effects of machining errors on the vortex torque of externally

---

*Corresponding author. Tel.: +86-451-86413840.
E-mail address: ycliang@hit.edu.cn

Foundation item: National Science Fund for Distinguished Young Scholars (50925521)

1000-9361 © 2011 Elsevier Ltd. Open access under CC BY-NC-ND license.
doi: 10.1016/S1000-9361(11)60011-3

pressurized gas journal-thrust bearings with slot restrictors by using finite element method, and got some achievements in the research field of vortex torque. Since the magnitude of surface roughness is close to the thickness of gas film of the bearing, there inevitably are effects on the vortex torque to some extent. Then based on the previous works, this article studies the effects of surface roughness on vortex torque in the presence of machining errors of air supported gyroscope, and accordingly guides the designing and manufacturing of air supported gyroscope.

2. Theoretical Basis

2.1. Reynolds equation and consistency transformation

The air supported gyroscope consists of journal and thrust bearing, and its structure diagram is showed in Fig.1. In Fig.1, R is bearing radius, L bearing length, L_1 half L, h_0 film thickness, a_0 slit width, b_0 axial clearance, h_b clearance of throttle circle, R_a radius of slit, R_{b1} inner radius of throttle circle, R_{b2} outer radius of throttle circle, p_0 air supply pressure, p_a atmospheric pressure. Several parts of gas film domain are of different forms that are annulus and cylinder, so it is difficult to program identically and to solve Reynolds equation. Then by using dimensionless and consistency transformation method[9], different domains of slit, journal and thrust parts are changed into uniform rectangular domain in this article. The new domains after consistency transformation we obtain are shown in Fig.2, where A_1 and A_2 are slit domains; H_1, H_2 and H_3 journal domains; B_1 and B_2 thrust domains; S_{a1} and S_{a2} air supply boundaries; S_{b1} and S_{b2} atmospheric boundaries; S_{ha1}, S_{ha2}, S_{hb1} and S_{hb2} intersections of different domains; ξ is unfolded gas film thickness direction; φ unfolded circumferential direction; ζ axial direction; o and o' points generated from the same point on bearing surface.

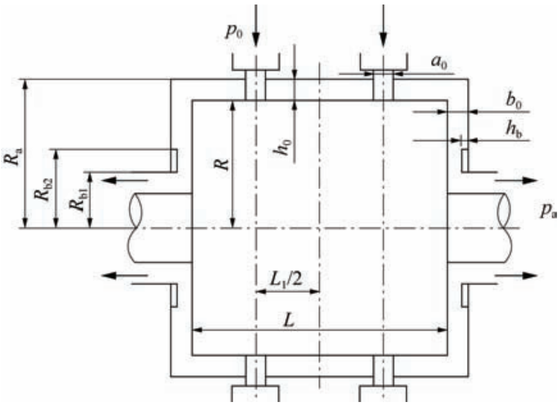

Fig.1 Structure of air supported gyroscope.

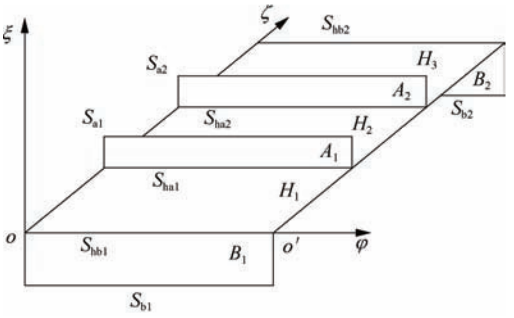

Fig.2 Domains after consistency transformation.

Reference quantities used in dimensionless method: R is the reference length, p_0 the reference pressure, and h_0 the reference film thickness.

Coordinates in consistency transformation method: x is the axial coordinate ($x \in [0, 2R]$), z the circumferential coordinate after journal film domain stretched into plane surface ($z \in [0, 2\pi R]$), φ the central angle coordinate of slit and thrust domain ($\varphi \in [0, 2\pi]$), and r the radial coordinate.

Principles of consistency transformation method: in the journal domain, $\zeta = x/R$, $\varphi = z/R$ and dimensionless journal gas film thickness $\bar{h} = h/h_0$; in the slit and thrust domains, $\zeta = \ln(r/R)$ and φ remains constant.

The obtained Reynolds equation is

$$\frac{\partial}{\partial \zeta}\left(\bar{h}^3 \frac{\partial \bar{f}}{\partial \zeta}\right) + \frac{\partial}{\partial \varphi}\left(\bar{h}^3 \frac{\partial \bar{f}}{\partial \varphi}\right) = 0 \tag{1}$$

where $\bar{f}$ is dimensionless pressure square.

2.2. Reynolds equation with surface roughness

Dimensionless film thickness of air supported gyroscope is a random quantity under the influence of surface roughness. It consists of two parts that are constant part and random part expressed as

$$\bar{h} = \bar{h}_0(\zeta, \varphi) + \bar{h}_s(\zeta, \varphi) \tag{2}$$

where $\bar{h}_0$ is the nominal dimensionless film thickness and $\bar{h}_s$ the random dimensionless film thickness variation caused by surface roughness.

Then the performance such as pressure distribution and gas flow rate will be random quantity. However, the things we concern with are the global contributions of surface roughness. So we can use mathematical expectation to calculate the average value of surface roughness, then solve the Reynolds equation and analyze the effects of surface roughness on the vortex torque of air supported gyroscope.

Taking the expectation values of both sides of Eq.(1), we get

$$\frac{\partial}{\partial \zeta}\left(E\left(\bar{h}^3 \frac{\partial \bar{f}}{\partial \zeta}\right)\right) + \frac{\partial}{\partial \varphi}\left(E\left(\bar{h}^3 \frac{\partial \bar{f}}{\partial \varphi}\right)\right) = 0 \tag{3}$$

where $E(\cdot) = \int_{-\infty}^{+\infty} (\cdot) f(h_s) \mathrm{d}h_s$ is expectation operator, h_s random journal gas film thickness and $f(h_s)$ probability density function expressed as

$$f(h_s) = \begin{cases} \dfrac{35}{32c^7}(c^2 - h_s^2)^3 & -c < h_s < c \\ 0 & \text{Otherwise} \end{cases} \tag{4}$$

where c is half the peak-to-valley height of surface roughness.

The direction diagram of surface roughness is shown in Fig.3, and the left and right diagram represent longitudinal and transverse surface roughness respectively. On the basis of Reynolds equation containing surface roughness[10-16], we obtain the Reynolds equation of air supported gyroscope in the presence of surface roughness.

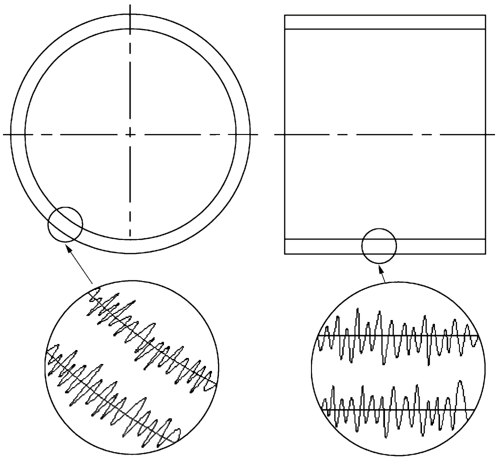
(a) Longitudinal (b) Transverse

Fig.3 Diagram of roughness direction.

When there is transverse surface roughness, the new Reynolds equation is

$$\frac{\partial}{\partial\zeta}\left(\frac{\partial\overline{f}}{\partial\zeta}\cdot\frac{1}{E(1/\overline{h}^3)}\right)+\frac{\partial}{\partial\varphi}\left(\frac{\partial\overline{f}}{\partial\varphi}\cdot E(\overline{h}^3)\right)=0 \tag{5}$$

where

$$\begin{cases}E(\overline{h}^3)=\overline{h}^3+\dfrac{1}{3}\overline{h}\,\overline{c}^2\\ \dfrac{1}{E(1/\overline{h}^3)}\approx\overline{h}^3-\dfrac{2}{3}\overline{h}\,\overline{c}^2\end{cases}$$

When there is longitudinal surface roughness, the new Reynolds equation is

$$\frac{\partial}{\partial\zeta}\left(\frac{\partial\overline{f}}{\partial\zeta}\cdot E(\overline{h}^3)\right)+\frac{\partial}{\partial\varphi}\left(\frac{\partial\overline{f}}{\partial\varphi}\cdot\frac{1}{E(1/\overline{h}^3)}\right)=0 \tag{6}$$

Solving the new Reynolds equation shown above, pressure distribution in the air supported gyroscope containing surface roughness information will be obtained, then we can analyze the effects of surface roughness on vortex torque of air supported gyroscope.

2.3. Reynolds equation discretization

The so-called discretization is just a transformation of the identical Reynolds equation from partial differential form into lumped parameter equation, and a further transformation of lumped parameter equation into algebraic equation by using the finite element method, in order to be used in analysis process easily[17]. Liu[17] studied the finite element method of the Reynolds equation discretization, and his works provided some facilities to solve the equations. On the basis of predecessors' works, by using triangular element, this article discretizes the identical Reynolds equation which consists of journal, thrust and slit parts. Finite element meshes are shown in Fig.4. The slit domain, journal domain and thrust domain are denoted clearly, and they represent the slit gas film, journal gas film and thrust gas film respectively. The equations according to the pressure square of all nodes are expressed as

$$\boldsymbol{KF}=\boldsymbol{T} \tag{7}$$

where $\boldsymbol{K}$ is stiffness matrix, $\boldsymbol{F}$ pressure square matrix, $\boldsymbol{T}$ constant matrix.

$$\begin{cases}\boldsymbol{K}=\displaystyle\sum_{e\subset H_1+H_2+H_3+A_1+A_2+B_1+B_2}\boldsymbol{Q}_{\mathrm{e}}^{\mathrm{T}}\frac{\boldsymbol{c}_{\mathrm{e}}\boldsymbol{c}_{\mathrm{e}}^{\mathrm{T}}+\boldsymbol{b}_{\mathrm{e}}\boldsymbol{b}_{\mathrm{e}}^{\mathrm{T}}}{4A_{\mathrm{e}}^2}G_{\mathrm{e}}\boldsymbol{Q}_{\mathrm{r}}\\ \boldsymbol{T}=-\displaystyle\sum_{e\subset H_1+H_2+H_3+A_1+A_2+B_1+B_2}\boldsymbol{Q}_{\mathrm{e}}^{\mathrm{T}}\frac{\boldsymbol{c}_{\mathrm{e}}\boldsymbol{c}_{\mathrm{e}}^{\mathrm{T}}+\boldsymbol{b}_{\mathrm{e}}\boldsymbol{b}_{\mathrm{e}}^{\mathrm{T}}}{4A_{\mathrm{e}}^2}G_{\mathrm{e}}\boldsymbol{Q}_{\mathrm{rb}}\boldsymbol{F}_{\mathrm{b}}\end{cases}$$

where e represents finite element, $\boldsymbol{c}_{\mathrm{e}}$ and $\boldsymbol{b}_{\mathrm{e}}$ are element coefficients, $\boldsymbol{Q}_{\mathrm{r}}$ and $\boldsymbol{Q}_{\mathrm{rb}}$ relational matrixes, A_{e} is element area, the expression of G_{e} is as follows:

$$G_{\mathrm{e}}=\begin{cases}\displaystyle\iint_e\overline{h}^3\mathrm{d}\varphi\mathrm{d}\zeta & e\subset H_1+H_2+H_3\\ \displaystyle\iint_e\overline{a}^3\mathrm{d}\varphi\mathrm{d}\zeta & e\subset A_1+A_2\\ \displaystyle\iint_e\overline{b}^3\mathrm{d}\varphi\mathrm{d}\zeta & e\subset B_1+B_2\end{cases}$$

where $\overline{a}$ and $\overline{b}$ are dimensionless slit width and dimensionless axial clearance.

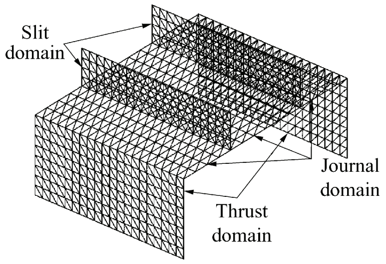

Fig.4 Finite element meshes.

2.4. Vortex torque calculation

Since the gas film thickness is so small compared with the length and diameter of the float, we can spread the journal gas film into plan surface in Cartesian coordinate system. y axis represents gas film thickness direction, z axis represents circumferential direction after spread. In other words, x, y and z replaced ζ, ξ and φ hereafter, in order to be used conveniently.

Along z axis, the gas motion equation is described as

$$\frac{\partial p}{\partial z}=\eta\frac{\partial^2 w}{\partial y^2} \tag{8}$$

where p is the gas pressure, η the gas viscosity coefficient and w circumferential velocity of gas flow.

By integrating Eq.(8), we have

$$w=\frac{1}{2\eta}\left(\frac{\partial p}{\partial z}\right)y^2+C_1y+C_2 \tag{9}$$

where C_1 and C_2 are integral constants.

The gas velocity on journal surface and bearing surface are zero, which implies that

$$w_{(y=0)}=w_{(y=h)}=0 \tag{10}$$

Substituting Eq.(10) into Eq.(9), we can get

$$\left.\begin{aligned} C_1&=-\frac{1}{2\eta}\left(\frac{\partial p}{\partial z}\right)h \\ C_2&=0 \end{aligned}\right\} \tag{11}$$

Then substituting Eq.(11) into Eq.(9), we get

$$w=\frac{1}{2\eta}\left(\frac{\partial p}{\partial z}\right)(y^2-hy) \tag{12}$$

The gas frictional stress formula is

$$\tau=\eta\frac{\mathrm{d}w}{\mathrm{d}y} \tag{13}$$

where τ is viscous stress.

Substituting Eq.(12) into Eq.(13), we can get

$$\tau=\frac{1}{2}\left(\frac{\partial p}{\partial z}\right)(2y-h) \tag{14}$$

The frictional force on the journal surface is

$$\tau=-\frac{1}{2}\left(\frac{\partial p}{\partial z}\right)h \tag{15}$$

From consistency transformation, we can get

$$z=R\varphi \tag{16}$$

And from discretization, we can get

$$\frac{\partial p}{\partial z}=\frac{\partial p}{R\partial\varphi}=\frac{\Delta p}{R\Delta\varphi} \tag{17}$$

where Δp and $\Delta\varphi$ are the pressure difference and the phase difference between adjacent nodes in the circumferential direction respectively.

Then substituting Eq.(17) into Eq.(15), we can get

$$\tau=-\frac{1}{2}\left(\frac{\Delta p}{R\Delta\varphi}\right)h \tag{18}$$

By integrating Eq.(8) in the whole journal domain and by the discretization, we can get the expression of total circumferential force shown as

$$F_\tau=\sum_{e\subset H_1+H_2+H_3} p_0Rh_0\frac{\Delta\bar{p}}{4\Delta\varphi}\iint_e \bar{h}\,\mathrm{d}\varphi\mathrm{d}\xi \tag{19}$$

where $\Delta\bar{p}$ is dimensionless pressure difference between adjacent nodes in the circumferential direction.

Eventually, the expression of vortex torque of air supported gyroscope is obtained:

$$T=\sum_{e\subset H_1+H_2+H_3} p_0R^2h_0\frac{\Delta\bar{p}}{4\Delta\varphi}\iint_e \bar{h}\,\mathrm{d}\varphi\mathrm{d}\xi \tag{20}$$

2.5. Mathematical models of errors

From Reynolds equation, we can see that the gas film thickness of thrust, journal and slit parts influence the pressure square significantly. The gas film thickness is very small, so minute change of gas film thickness caused by machining errors will influence the stiffness matrix, and further influence the pressure distribution and vortex torque of air supported gyroscope. The machining errors affecting vortex torque significantly are introduced thereinafter. Their mathematical models are expressed as Eqs.(21)-(23), and their diagrams are shown as Figs.5-7.

Radial eccentricity is shown in Fig.5, where e_r represents radial eccentricity. And $\bar{h}$ is expressed as

$$\bar{h}=1+\varepsilon\cos\varphi \tag{21}$$

where ε is radial eccentricity ratio.

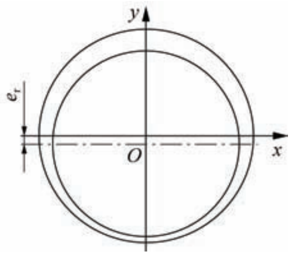

Fig.5 Diagram of radial eccentricity.

Oval error of journal is shown in Fig.6, and its dimensionless mathematical model is expressed as

$$\bar{h}=1+\frac{e_1}{2h_0}\cos(2\varphi-2\theta) \qquad 0\le\theta\le 2\pi \tag{22}$$

where e_1 is oval error of float and θ setting angle of float.

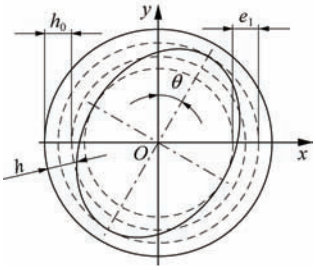

Fig.6 Diagram of oval error of float.

Tilting error of throttle slit is shown in Fig.7, and its dimensionless mathematical model is expressed as

$$\bar{a}=\frac{a_0+R\sin\alpha\cos(\varphi-\beta)\mathrm{e}^{\xi}}{h_0} \qquad 0\le\xi\le\ln\frac{R_\mathrm{a}}{R} \tag{23}$$

where α is tilting angle of throttle slit and β the tilting position of throttle slit. β is the angle between symmetry plane of slit domain (α is not equal to zero) and y axis.

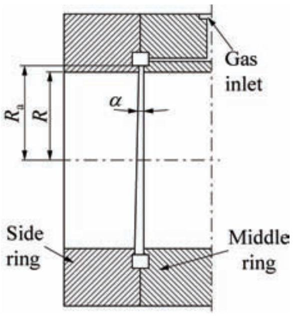

Fig.7 Diagram of tilting error of throttle slit.

3. Results and Discussion

This article analyzes the effects of surface roughness on vortex torque of air supported gyroscope, and the main parameters used in the research are shown in Table 1. In Table 1, D is bearing diameter.

Table 1 Parameters of air supported gyroscope

Parameter	Data
Air supply pressure : Atmospheric pressure (p_0/p_a)	3.0
Diameter of slit outer margin : Diameter of float (D_s/D)	1.057
Bearing length : Diameter of float (L/D)	1
Diameter of throttle boss : Diameter of float (D_t/D)	0.486
Slit width : Film thickness : Clearance of throttle circle ($a_0 : h_0 : h_b$)	0.389 : 1 : 2.722
Oval error of float/μm	1
Tilting error of throttle slit/μm	1
Setting angle of float/(°)	45

The film thickness of thrust part is much larger than surface roughness, so its effects on vortex torque are ignored. In order to be convenient for analysis, surface roughness of journal and slit parts are respectively defined as

$$R_{aj} = n_j a_0 \qquad n_j = 0.05, 0.06, \cdots, 0.15 \tag{24}$$

$$R_{as} = n_s a_0 \qquad n_s = 0.05, 0.06, \cdots, 0.15 \tag{25}$$

where n_j and n_s are reference quantities of surface roughness.

When n_s is equal to 0.15, effects of journal surface roughness on vortex torque are analyzed in different sizes and directions. Then the curves are shown in Fig.8, in which the symbol Ld represents longitudinal direction, while the symbol Td represents transverse direction. It can be seen that neither the journal surface roughness size nor the direction influence vortex torque significantly. It is because journal film thickness is so large compared with journal surface roughness that effects of surface roughness are weakened in Reynolds equation. Mathematical expectation of film thickness is not enormously changed by surface roughness, so the curves have little variation.

Since journal surface roughness affects vortex torque insignificantly, effects of slit surface roughness on vortex torque are analyzed in different sizes and directions, only when n_j equals 0.15 and journal surface roughness is longitudinal, in order to reduce computation time. The vortex torque curves are shown in Fig.9 from which it can be seen that slit surface roughness affects vortex torque significantly. Longitudinal surface roughness makes vortex torque larger, while transverse surface roughness makes vortex torque smaller. The reason is that slit gas film thickness is very small and close to surface roughness. Then the effects of surface roughness are very significant in Reynolds equation. In other words, mathematical expectation of film thickness is changed by surface roughness significantly. Furthermore the pressure distribution of the whole gas film domain is changed by the variation of surface roughness magnitude and direction. Then vortex torque is influenced.

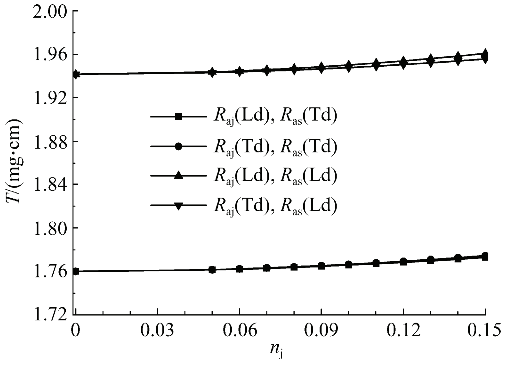

Fig.8 Influence of journal surface roughness.

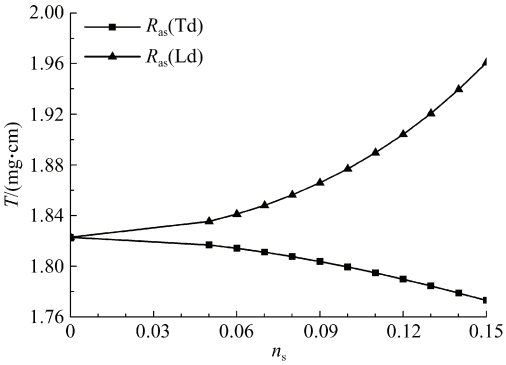

Fig.9 Influence of slit surface roughness.

When slit surface roughness is of the same magnitude and different directions, the relative change rate of vortex torque (R_t) is analyzed and the curve is shown in Fig.10. It increases with increasing n_s. It approaches 1% with n_s equal to 0.05, and approaches 10.6% with n_s equal to 0.15. In other words, small variation of surface roughness will cause great change of vortex torque, when surface roughness is relatively large. The reason is that different surface roughness directions cause the mathematical expectation of film thickness larger and smaller respectively and further influence the relative change rate of vortex torque.

In the domain analyzed in this article, the maximal value and the minimal value are

$$\begin{cases} T_{max} = 1.96 \text{ mg} \cdot \text{cm}, \text{when } n_s = 0.15 \text{ (Ld) and } n_j = 0.15 \\ T_{min} = 1.76 \text{ mg} \cdot \text{cm}, \text{when } n_s = 0.15 \text{ (Td) and } n_j = 0.05 \end{cases}$$

The difference between them approaches 11.4%.

To conclude, the surface roughness has effects on vortex torque of air supported gyroscope to some extent. On the basis of machining errors control, surface roughness magnitude and direction should be controlled properly. In practice, there are many factors affecting vortex torque, and surface roughness is only one of them. Therefore it is too difficult to distinguish the effects of surface roughness. However, taking account of surface roughness indeed helps to control vortex torque in the manufacturing of air supported gyroscope.

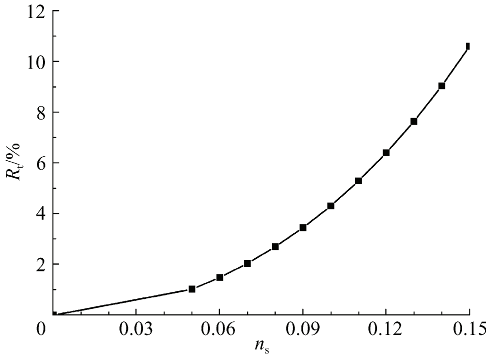

Fig.10 Relative change rate of vortex torque.

4. Conclusions

(1) On the basis of Christensen's rough surface stochastic model and by using finite element method, the correction terms in Reynolds equation are obtained and the effects of surface roughness on vortex torque of air supported gyroscope are analyzed.

(2) It is shown that journal surface roughness size and direction affect vortex torque insignificantly, while slit surface roughness affects vortex torque significantly. Longitudinal slit surface roughness makes vortex torque larger, while transverse slit surface roughness makes vortex torque smaller.

(3) The difference between the maximal vortex torque and the minimal one approaches 11.4% during the range analyzed in this article. So size and direction of surface roughness should be properly controlled in real production in order to control vortex torque of air supported gyroscope.

References

[1] Lu Y J. Inertial device. Beijing: Astronautic Publishing House, 1990. [in Chinese]

[2] Wu M J, Yi W K, Zhou A S. Inertial device manufacturing technology. Beijing: Astronautic Publishing House, 1991. [in Chinese]

[3] Wang B L, Liu J M, Xu Z Q. Measuring turbine torque of hydrostatic fluid bearing by using image process. Missiles and Space Vehicles 2005(5): 43-47. [in Chinese]

[4] Lu Y J. Gyroscope and inertial navigation principle. Beijing: Science Press, 1964. [in Chinese]

[5] Yao Y X, Du J J, Liu D, et al. Numerical analysis of manufacturing error influence on vortex torque of externally pressurized gas bearings. Acta Aeronautica et Astronautica Sinica 2003; 24(2): 124-128. [in Chinese]

[6] Du J J, Yao Y X, Gao D, et al. A numerical analysis of vortex torque of externally pressurized gas journal-bearings. Lubrication Engineering 2005(3): 57-59. [in Chinese]

[7] Liu J S, Sun Y Z, Lu L H, et al. Manufacturing errors effects on disturbing torque of aerostatic bearings. Applied Mechanics and Materials 2009; 16-19: 505-509.

[8] Liu J S, Sun Y Z, Lu L H, et al. Factors effect on vortex torque of aerostatic bearings. Advanced Materials Research 2010; 97-101: 3745-3748.

[9] Liu D, Du J J, Yao Y X, et al. Discretization and consistent conditions of lubrication equations for externally pressurized gas bearings with slot restrictors. Chinese Journal of Mechanical Engineering 2003; 39(1): 33-37. [in Chinese]

[10] Christensen H. Stochastic models for hydrodynamic lubrication of rough surfaces. Tribology Group 1969; 184(1): 1013-1026.

[11] Pande S S, Somasundaram S. Effect of manufacturing errors on the performance of aerostatic journal bearings. Wear 1981; 66(2): 145-156.

[12] Lin J R. Surface roughness effect on the dynamic stiffness and damping characteristics of compensated hydrostatic thrust bearings. International Journal of Machine Tools and Manufacture 2000; 40(11): 1671-1689.

[13] Lin J R, Hsu C H, Lai C. Surface roughness effects on the oscillating squeeze-film behavior of long partial journal bearings. Computers and Structures 2002; 80(3-4): 297-303.

[14] Chiang H L, Hsu C H, Lin J R. Lubrication performance of finite journal bearings considering effects of couple stresses and surface roughness. Tribology International 2004; 37(4): 297-307.

[15] Nagaraju T, Sharma S C, Jain S C. Study of orifice compensated hole-entry hybrid journal bearing considering surface roughness and flexibility effects. Tribology International 2006; 39(7): 715-725.

[16] Nagaraju T, Sharma S C, Jain S C. Influence of surface roughness on non-Newtonian thermohydrostatic performance of a hole-entry hybrid journal bearing. Journal of Tribology 2007; 129(3): 595-602.

[17] Liu D, Liu Y H, Chen S J. Aerostatic gas lubrication. Harbin: Harbin Institute of Technology Press, 1990. [in Chinese]

Biographies:

LIANG Yingchun Born in 1964, Ph.D., he is a professor and dean of School of Mechatronics Engineering, Harbin Institute of Technology. His main research interest is precision and ultra-precision machining technique.
E-mail: ycliang@hit.edu.cn

LIU Jingshi Born in 1982, he received B.S. and M.S. degrees from Harbin Institute of Technology. He is a Ph.D. candidate of Harbin Institute of Technology. His main research interest lies in air bearing.
E-mail: ljshhh@sina.com